International Journal of Technology
http://ijtech.eng.ui.ac.id

Research Article

Controlling-Based Optimization Framework for Dynamic Grid Reconfiguration: Enhancing Resilience and Cost-Efficiency in Hybrid Renewable Microgrids with Peer-to-Peer Energy Trading

Ghaith M. Fadhil[1,2*], Saeid Ghassem Zadeh[1], Sina Roudnil[1]

[1]Faculty of Electrical and Computer Engineering, University of Tabriz, 29 Bahman boulevard, Tabriz, Iran, 51666-16471,

[2]Civil Engineering Department, College of Engineering, Al-Qasim Green University, Babylon 51013, Iraq

[*]Corresponding author: Kaithmajed@wrec.uoqasim.edu.iq; Tel.: +964 772 511 6409; Fax: +98 41-33340081

Abstract: This study proposes an advanced framework for combining renewable energy resources with adaptive feeder restructuring to improve both local energy exchange and power system resilience. Instead of conventional supply driven operation, the model emphasizes the coordinated placement of solar photovoltaic (PV) units and wind turbines (WTs), along with intelligently optimized grid reconfiguration using Particle Swarm Optimization (PSO), is the best strategy for operating modern electricity microgrids. A distinctive feature of the design is the integration of a peer-to-peer (P2P) market, which allows prosumers within the microgrid to negotiate power transactions in real time, thereby further increasing trading efficiency and reducing reliance on the main grid. A multi-stage analysis method is used to compare three different system configurations: a baseline scenario of energy distribution with PV cells and renewable energy integration, a scenario integrating hybrid PV-WT, and a fully integrated PV-WT system with optimized grid reconfiguration. The Taiwan Power Company (TPC) distribution test system served as the benchmark for assessing critical indicators, such as voltage regulation, power loss, and cost of operation. The results show that the coordinated approach of feeder restructuring with P2P trading reduces network losses from 0.0024 to 0.002 MW and lowers the average operating cost from 2.3729 \$/MWh to 1.954 \$/MWh. This methodology provides a scalable and resilient solution for enabling secure, affordable, and sustainable electricity exchange in future smart distribution grids.

Keywords: Distribution network reconfiguration; Energy trading; Power loss reduction; Renewable energy integration; Smart grid

1. Introduction

1.1 Motivation

The widespread adoption of distributed energy technologies, such as solar PV panels and wind turbines, is changing the operation of modern grids. When combined with peer-to-peer (P2P) electricity trading frameworks, these resources enable prosumers to directly exchange surplus generation across local networks (Huo et al., 2024). Unlike traditional centralized markets, P2P trading employs decentralized digital infrastructures, often supported by blockchain platforms, to conduct secure and transparent transactions (Guzmán-Henao et al., 2024). This transformation enhances grid flexibility, strengthens system resilience, and increases overall market efficiency (Mokaramian et al., 2024), (Roudnil et al., 2025a; Roudnil et al., 2025b; Roudnil et al., 2025c).

To ensure the reliable operation of such decentralized microgrids, the network configuration must be continually adapted. This is commonly termed topology adjustment or network

https://doi.org/10.14716/ijtech.v17i2.8034
Received August 2025; Revised October 2025; Accepted January 2026

restructuring and is often referred to as network reconfiguration (C. Zhang et al., 2021). Distribution Network Reconfiguration (DNR) is defined as a switch-based topology optimization process in which the open/closed states of sectionalizing and tie switches are systematically altered to obtain an optimal radial network structure. Unlike simple feeder rerouting, DNR explicitly considers binary switch decision variables, power flow constraints, voltage limits, and radiality conditions to minimize power losses, improve voltage profiles, and reduce operational costs without modifying the network's physical (Wongthongtham et al., 2021). The problem is inherently complex, which has encouraged researchers to apply advanced metaheuristic optimization techniques for determining effective switching strategies (Jogunola et al., 2024; Hafeez et al., 2020). Nevertheless, renewable energy sources (RESs) add uncertainty due to their variability (Soto et al., 2021). This unpredictability challenges the dependability and efficiency of P2P-based systems. Heuristic optimization approaches, particularly particle swarm–based strategies, have been explored as promising tools for integrating renewables into decentralized trading environments (B. Zhou et al., 2021)

1.2 Literature review

The body of work on hybrid microgrids integrating renewable energy sources has grown extensively. Most contributions have focused on achieving cost efficiency, fair resource allocation, and secure data handling in energy storage–based systems (Keck et al., 2019), (Roudnil et al., 2025a; Roudnil et al., 2025b; Roudnil et al., 2025c). Several studies have improved demand-side management in stand-alone PV systems (Albadi and El-Saadany, 2008), developed adaptive controllers for hybrid renewable integration (Jiang et al., 2013), designed versatile management schemes for MGs (Serra, 2025), and introduced cooperative frameworks with shared storage for grid-connected operation (Lv and Ai, 2016). Optimization techniques, with PSO as a popular tool, have been used to minimize operational expenses and address demand–supply imbalances (Chen et al., 2021).

PSO is a population-based metaheuristic algorithm inspired by the collective behavior of social organisms, where candidate solutions (particles) iteratively update their positions in the search space based on individual experience and global best knowledge. PSO is widely adopted in power system optimization because of its simplicity, low computational burden, and strong global search capability. However, classical PSO may suffer from premature convergence, limited exploration–exploitation balance, and inadequate handling of complex constraints, particularly in highly nonlinear and mixed-integer problems such as distribution network reconfiguration and energy trading. Consequently, enhanced PSO variants incorporating adaptive inertia weights, penalty-based constraint handling, and convergence improvement mechanisms have been developed to ensure solution feasibility, robustness, and faster convergence. Variants such as the Walrus PSO have been applied to reduce voltage instability and operational risks under renewable intermittency (C. Wang et al., 2021; Soroudi and Amraee, 2013). Similarly, PSO has been leveraged to optimize the configuration of hybrid PV-WT farms, resulting in lower losses and better voltage support (Thakar et al., 2019). An improved PSO algorithm for integrating renewable energy sources was developed by Manoz et al., 2025.

The PSO model ensures optimal planning of PV and WT farms to minimize system losses by incorporating multiple units and inverters. Other recent research has indicated that sustainability, resilience, and efficiency can be improved in multiple ways by improving energy system operations and integrating hybrid renewable energy sources (Ergun et al., 2025). An advanced PSO algorithm for distributed energy systems combining demand information with a diverse generation source developed [Trinka1.1] by the authors in (W. Zhang et al., 2025), the objectives were to reduce operating costs and energy fluctuations. Xiao et al., 2017 presented a novel optimization algorithm to optimize the variant market conditions of distributed energy resources, with the objectives of maximizing the incomes and improving the flexibility of the system. A novel gray wolf-based PSO hybrid optimization was introduced by Y. Xu et al., 2020 that depends on multistage bidding strategies to enhance the performance of smart MGs and virtual power plant profitability.

Predictive models of CO_2 emissions and carbon allocation systems utilizing PSO-enhanced neural networks are also part of the effort to match power grids with peak carbon targets (Feijoo and Das, 2015). Additionally, a hybrid optimization model integrating deep learning and an enhanced PSO algorithm is suggested to address multi-objective problems in distributed power generation systems, emphasizing reliability, environmental benefits, and economic efficiency (W. Zhang et al., 2025). A model for integrated bidding and battery scheduling was proposed to enable sealed-bid double auction power trading with peer microgrids, effectively handling uncertainty (Zubin et al., 2025). Another study focused on an uncertainty-aware day-ahead scheduling approach for microgrids that accounts for response fatigue using an IGDT method (Tostado-Véliz et al., 2022). The use of uncertainty-aware model predictive control for residential buildings participating in intraday markets was also investigated to optimize energy usage (Tarnate et al., 2022). Research has been conducted on the uncertainty-aware deployment of mobile energy storage systems, which involves network reconfiguration, to ensure distribution grid resilience (Nazemi et al., 2021). Separately, a forecasting method was developed using stacking-ensemble feature selection and self-supervised learning for precision and uncertainty-aware steam flow (H. Zhou et al., 2025; F. Zhou and Yu, 2025). A hybrid stochastic-robust optimization model was introduced for resiliency-oriented scheduling for multi-microgrids, which includes network reconfiguration and uncertainty management (Zare et al., 2024), (Roudnil et al., 2025a; Roudnil et al., 2025b; Roudnil et al., 2025c).

An uncertainty-aware critic augmentation technique was proposed for hierarchical multi-agent EV charging control, specifically addressing distribution network constraints (Pang et al., 2024). Additionally, a deep learning-based demand response framework was developed for the short-term operation of renewable-based microgrids under uncertainty (Gharehveran et al., 2024). Moving edge concept was introduced in an uncertainty-aware approach for on-demand edge computing, which can be interpreted as a form of optimal scheduling with network constraints and reconfiguration (F. Zhou and Yu, 2025). For distribution networks, the uncertainty-aware optimal placement of capacitors and DSTATCOM to reduce losses and voltage deviations has been the focus of research (Alanazi et al., 2025). An uncertainty-aware multi-agent deep reinforcement learning approach was presented for robust active voltage control, aiming to maintain voltage profiles and mitigate network violations (Liu et al., 2025). An uncertainty-aware economic dispatch model for integrated energy systems, considering demand response and carbon-emission costs (Y) was also proposed. (W. Zhang et al., 2025; Y. Zhang et al., 2025). A data-driven stochastic planning method was developed to address uncertainty to enable network-constrained energy sharing in microgrids (X. Zhang et al., 2024). The optimal scheduling of multi-use battery storage systems under uncertainty has also been investigated (Lechl et al., 2025), as has the coordinated dispatch of electric, thermal, and hydrogen vectors in microgrids under uncertainty using a constrained optimization method (C. Xu and Abdalla, 2026). An uncertainty-aware optimal dispatch framework was created for a multi-energy hub, focusing on emissions and managing uncertainty from renewable sources and load demand (Sharma and Pindoriya, 2024). The stochastic allocation and management of soft open points have also been explored to reduce harmonic distortion, voltage deviations, and losses in distribution networks under uncertainty, which is a form of reconfiguration (Ebrahimi et al., 2025). A novel method using uncertainty-aware knowledge transformers and multi-agent reinforcement learning was proposed for peer-to-peer energy trading (Ibad et al., 2025). For energy optimization in microgrids, a deep deterministic policy gradient method was introduced to handle the uncertainty from renewable energy generation and load forecasting (T. Wang et al., 2025). Furthermore, an uncertainty-aware optimal energy management model was developed for smart distribution networks to ensure voltage stability (Gangil et al., 2025), and an energy management strategy was proposed for microgrids with integrated electric bicycle charging stations and a green certificate market, considering uncertainty and network constraints (Shayeghi and Faraji Davoudkhani, 2025).

1.3 Problem statement

Despite notable advancements in distributed energy systems and peer-to-peer (P2P) trading, several challenges remain unresolved. Although various energy management strategies have been developed to integrate renewable energy sources (RESs), such as photovoltaic (PV) and wind power (WT), most approaches struggle to address the uncertainty inherent in these resources. Optimization techniques, including particle swarm optimization (PSO) and its variants, have been applied to mitigate uncertainty and reduce costs; however, such methods often rely on worst-case assumptions, leading to overly conservative decisions that are not always practical in real-world contexts. In addition, current P2P trading models frequently neglect the distribution network's physical constraints. While some studies examine network reconfiguration for system stability and others focus on P2P market design, integrated solutions that account for both remain limited. This lack of coordination can result in impractical scheduling and trading outcomes, thereby undermining the efficiency and resilience of the system. The literature clearly points to a gap in research that simultaneously addresses P2P energy trading, DNR, and the uncertainty associated with RES integration.

Most studies have investigated these aspects in isolation or only partially. Although P2P energy trading enhances market efficiency and local energy utilization, neglecting physical power system constraints can lead to unsafe operating conditions. To ensure electrical feasibility, practical P2P trading models must explicitly incorporate network constraints such as bus voltage limits, line current (thermal) limits, and power flow equations. Without these constraints, trading decisions may result in voltage violations, line overloading, and unrealistic energy exchanges that cannot be realized in actual distribution networks. Therefore, coupling P2P market mechanisms with power system–aware optimization is essential to guarantee energy trading outcomes that are secure, reliable, and physically implementable. Therefore, a holistic framework that optimizes trading strategies, ensures physical feasibility through dynamic network reconfiguration, and effectively manages the operational and economic impacts of renewable uncertainty is needed. This study aims to fill this gap by proposing an integrated optimization framework.

1.4 Research contribution

This study provides several key contributions to decentralized energy management and distribution network optimization, directly addressing the research gaps identified in the literature: (1) Development of a Novel PSO-Based Optimization Framework for P2P Energy Trading: This study introduces a PSO-driven optimization framework specifically designed for electricity distribution networks engaged in P2P energy trading among interconnected microgrids. This framework is designed to holistically address operational and economic objectives within a decentralized energy paradigm. (2) Comprehensive Scenario-Based Analysis on the TPC Network: This research conducts a rigorous, multi-scenario operational analysis using real-world data from the TPC electricity distribution network for P2P trading. This includes establishing a crucial baseline scenario representing the TPC networks with PV integration operation and using optimization techniques to find the best power lines and locations for PV, against which all subsequent advancements are quantitatively compared. (3) Optimal RE integration and grid reconfiguration: This research aims to study the impact of integrating RE sources into electricity grids using different approaches. The TPC grid operation will be modeled with PV and WT. Then, with the help of the dynamic grid reconfiguration, we will employ the proposed PSO optimization algorithm to determine the optimum locations of the grid switch. (4) The Impact of Reconfiguration on Peer-to-Peer Energy Trading: A 24-hour P2P energy trading operation will be comprehensively modeled for the hybrid renewable energy integrated TPC grid. The performance of energy trading (with and without reconfiguration) will be compared.

The remainder of this paper is organized as follows: Section 2 outlines the simulation design and case study scenarios. Section 3 introduces the methods, including system modeling, PSO algorithm, and IEEE 84-bus TPC network representation. Section 4 presents the results and discussion. Section 5 discusses the findings in a broader context and, concludes and points to future research opportunities.

2. Methods

2.1 Mathematical formulation

The optimization framework is designed to achieve two interdependent goals: reducing operational expenditure and ensuring efficient PEPTs. The formulation integrates a penalty on variability to account for uncertainty in renewable energy generation, thereby encouraging solutions that are not only economical but also resilient to fluctuations in solar and wind production. The overall objective function can be expressed as follows:

$$\min \left(\sum_{i=1}^{N} C_i(x_i) + \lambda \cdot \mathrm{Var}(\Delta P_{RE}) \right) \tag{1}$$

Where $C_i(x_i)$: Total Operational Cost (Generation Cost, Switching Cost, and grid power purchase) for each microgrid or participant, λ: Weight factor for the uncertainty variance penalty, and $\mathrm{Var}(\Delta P_{RE})$: Variance of the uncertainty in renewable energy. The renewable output is modeled as a nominal forecast plus a stochastic deviation:

$$P_{RE} = \bar{P}_{RE} + \Delta P_{RE} \tag{2}$$

2.1.1 Adding renewable energy to the MMG

The power generated by a solar PV system is given by the following:

$$P_{PV} = \eta_{PV} \cdot A \cdot G \cdot \cos(\theta) \tag{3}$$

The power output of a wind turbine is expressed as follows:

$$P_{\text{wind}} = \frac{1}{2} \cdot \rho \cdot A \cdot v^3 \cdot C_p \tag{4}$$

The mathematical formalism employed to simulate the operational characteristics of PV and WT generation units are of paramount importance in elucidating the functional role of distributed RE resources within the operational context of microgrids and MMG systems.

2.1.2 Constraints Imposed on Reconfiguration

The power balance, voltage limits, power flows, and radiality requirements constrain the reconfiguration problem, which are characterized by the following key equations:

2.1.3 Net power balance equations

Active power balance:

$$P_{k,t}^{\text{net}} = P_{k,t}^{b} + P_{k,t}^{L} + P_{k,t}^{L,drp} - P_{k,t}^{fc} + P_{k,t}^{el} - P_{k,t}^{L,shadded} \tag{5}$$

Reactive power balance:

$$Q_{k,t}^{\text{net}} = Q_{k,t}^{L} + Q_{k,t}^{L,drp} - Q_{k,t}^{L,shadded} \tag{6}$$

1. **Power flow constraints**

   For the active power:

$$P_{k,t}^{\text{net}} \geq P_{ik,t} - \sum_{j \in \mathcal{J}} P_{ik,t} - [1 - \gamma_{ik,t}] \cdot M \tag{7}$$

$$P_{k,t}^{\text{net}} \leq P_{ik,t} - \sum_{j \in \mathcal{J}} P_{ik,t} + [1 - \gamma_{ik,t}] \cdot M \tag{8}$$

For reactive power:

$$Q_{k,t}^{\text{net}} \geq Q_{ik,t} - \sum_{j \in \mathcal{J}} Q_{ik,t} - [1 - \gamma_{ik,t}] \cdot M \tag{9}$$

$$Q_{k,t}^{\text{net}} \leq Q_{ik,t} - \sum_{j \in \mathcal{J}} Q_{ik,t} + [1 - \gamma_{ik,t}] \cdot M \tag{10}$$

2. **Voltage Constraints**

   The voltage magnitude at bus k:

$$U_{k,t} \geq U_{i,t} - \frac{r_{ik} P_{ik,t} + x_{ik} Q_{ik,t}}{U_{1,t}} - [1 - \gamma_{k,t}] \cdot M \tag{11}$$

$$U_{k,t} \leq U_{i,t} - \frac{r_{ik} P_{ik,t} + x_{ik} Q_{ik,t}}{U_{1,t}} + [1 - \gamma_{k,t}] \cdot M \tag{12}$$

   Voltage limits:

$$U_i^{\min} \leq U_{i,t} \leq U_i^{\max} \tag{13}$$

3. **Flow Line Constraints**

   Active power flow:

$$-Y_{ik,t} \cdot P_{ik}^{\max} \leq P_{ik,t} \leq Y_{ik,t} \cdot P_{ik}^{\max} \tag{14}$$

   Reactive power flow:

$$-Y_{ik,t} \cdot Q_{ik}^{\max} \leq Q_{ik,t} \leq Y_{ik,t} \cdot Q_{ik}^{\max} \tag{15}$$

4. **Radial operation constraints**

   Spanning tree approach:

$$\beta_{ik,t} + \beta_{ik,t} = Y_{ik,t} \tag{16}$$

$$\sum_{k} \beta_{k0,t} = 0 \tag{17}$$

$$\sum_{k} \beta_{ki,t} \leq 1 \tag{18}$$

2.1.4 Power flow analysis

The solution of nonlinear equations in MMG networks relies on iterative techniques. For a general System, $f(x) = 0$, Newton-Raphson updates are applied as follows:

$$x^{(k+1)} = x^{(k)} - J^{-1}(x^{(k)}) \cdot f(x^{(k)}) \tag{19}$$

The power flow problem in MMGs involves solving the following nonlinear equations for active (P) and reactive (Q) power balances:

$$P_i = V_i \sum_{j}^{N} V_j (G_{ij} \cos \theta_{ij} + B_{ij} \sin \theta_{ij}) \tag{20}$$

$$Q_i = V_i \sum_{j}^{N} V_j (G_{ij} \sin \theta_{ij} - B_{ij} \cos \theta_{ij}) \tag{21}$$

2.1.5 Application of MMG optimization techniques

The optimization metric combines operating cost and resilience to account for renewable uncertainty in MMGs:

$$\text{Fitness}(x) = w \cdot \text{Cost}(x) + (1 - w) \cdot \text{Resilience}(x) \tag{22}$$

The fitness function used in an optimization technique for MMGs with the PSO approach. This function is designed to account for uncertainty by combining two objectives: minimizing cost (x) and maximizing resilience (x), with a weighting factor w to adjust their relative importance. In this study, the resilience criterion represents the microgrid's ability to maintain performance under the uncertainty of renewable energy generation. Resilience is quantified using a penalty-based formula that considers the buses' unconsumed energy resulting from load shedding and voltage range violations during the planning horizon. Therefore, higher values of load shedding and result in larger resilience penalties, indicating a decrease in system robustness. By including this criterion in Equation 22, the optimization process explicitly prefers solutions that minimize operational disturbances and constraint violations, thereby improving the distribution network's resilience under uncertain PV and wind generation.

The location of each new particle is determined by adding its velocity to its current location, which changes with each step. This method causes the particles to move around and search for the solution everywhere. Each particle determines its location based on its best finding and the best finding of all the other particles in the group. Each particle adjusts its location based on its velocity as follows:

$$x_i^{(t+1)} = x_i^{(t)} + v_i^{(t+1)} \tag{23}$$

In search algorithms, velocity evolves as a weighted combination of three factors: inertia, self-learning (cognitive term), and collective knowledge (social term), leveraging the collective's findings:

$$v_i^{(t+1)} = w \cdot v_i^{(t)} + c_1 \cdot r_1 \cdot (p_i^{\text{best}} - x_i^{(t)}) + c_2 \cdot r_2 \cdot (g^{\text{best}} - x_i^{(t)}) \tag{24}$$

This mechanism balances exploration and exploitation, enabling efficient convergence toward optimal scheduling solutions.

2.1.6 Cost Equations and Integration into Optimization Functions

To maintain the viability of decentralized energy trading, total operational expenses must be minimized while guaranteeing demand-supply equilibrium. Each microgrid's cost has three primary components: generation, trading, and penalties. The generation cost model can be written as follows:

$$C_{i,t}^{\mathrm{Gen}} = \lambda_i^{\mathrm{MT}} p_{i,t}^{\mathrm{MT}} + \lambda_i^{\mathrm{BS}} p_{i,t}^{\mathrm{BSC}} + p_{i,t}^{\mathrm{BD}} + k_i^{\mathrm{TS}} (H_{i,t}^{\mathrm{TSC}} + H_{i,t}^{\mathrm{TSD}}) \tag{25}$$

2.1.7 Peer-to-Peer

The energy balance equation plays a significant role in controlling energy requests and provision when considering P2P processes. In microgrid designs, the energy balance equation for electrical and thermal power in a multi-energy network given by the following:

$$P_{i,t}^{\mathrm{Ref}} = P_{i,t}^{\mathrm{D}} - P_{i,t}^{\mathrm{MT}} - P_{i,t}^{\mathrm{RES}} + P_{i,t}^{\mathrm{BSC}} - P_{i,t}^{\mathrm{BSD}} \tag{26}$$

$$H_{i,t}^{\mathrm{Ref}} = H_{i,t}^{\mathrm{D}} - H_{i,t}^{\mathrm{MT}} + H_{i,t}^{\mathrm{TSC}} - H_{i,t}^{\mathrm{BSD}} \tag{27}$$

The power balance equation for microgrid i under scenario s at time t is

$$P_{i,s,t}^{\mathrm{mt}} + P_{i,s,t}^{\mathrm{dis}} + P_{i,s,t}^{\mathrm{w}} + P_{i,t}^{\mathrm{ms}} = P_{i,t}^{\mathrm{load}} + P_{i,s,t}^{\mathrm{hs}} \tag{28}$$

2.1.8 PSO Optimization Function for P2P

The optimization function minimizes the total cost while satisfying supply-demand constraints. The optimization problem is solved using a distributed approach that combines ADMM and ATC.

$$\min F^{\mathrm{dh}} = (C^{\mathrm{ls}} + C^{\mathrm{sw}} + C^{\mathrm{its}}) \tag{29}$$

The P2P energy trading algorithm's parameters include important factors that determine the system's energy management and costs. The following are the key variables and their interactions: - The total energy supplied by a microgrid i. Represents the energy generated by local sources (e.g., renewable energy, microturbines, and battery storage) within microgrid i.

$$S_i = P_{i,t}^{\mathrm{MT}} + P_{i,t}^{\mathrm{RES}} + P_{i,t}^{\mathrm{BSC}} - P_{i,t}^{\mathrm{BSD}} \tag{30}$$

Total energy demand of microgrid i. Represents the total energy required to meet the load demand of microgrid i.

$$D_i = P_{i,t}^{\mathrm{D}} + H_{i,t}^{\mathrm{D}} \tag{31}$$

Energy exchanged between microgrid i and microgrid j. Represents the energy traded between microgrids and balance supply and demand.

$$e_{i,j,t}^{\mathrm{DN}} + e_{j,i,t}^{\mathrm{DN}} = 0 \tag{32}$$

Total costs of producing, selling, and purchasing electricity, plus any fines related to microgrids. The economic performance of microgrid i is evaluated by considering generation costs, trading costs, and penalties for unmet demand. The cost function for each agent participating in P2P energy trading is as follows:

$$C_i = \sum_{t \in N_T} (C_{i,t}^{\mathrm{Gen}} + C_{i,t}^{\mathrm{Bill}} + C_{i,t}^{\mathrm{Disc}} + C_{i,t}^{\mathrm{P2P}}) + C_{i,t}^{\mathrm{P2P}} \tag{33}$$

The cost function for microgrid i under uncertainty is as follows:

$$\min F_i^{\mathrm{ms}} = (1-\rho_i) \sum_{s \in \Omega_i} \sum_{j \in (M_u) \setminus i} \sum_{t \in \tau} \pi_{i,s} (C_{i,s}^{\mathrm{mt}} + C_{i,s}^{\mathrm{bs}} + C_{i,s}^{\mathrm{ws}} + C_{i,s}^{\mathrm{ex}} + C_{i,s}^{\mathrm{us}}) + \rho_i (\xi_i + \frac{1}{1-a_i} \sum_{s \in \Omega_i} \pi_{i,s} \delta_{i,s}) \tag{34}$$

The fitness function is a measure we use in computer programs (such as PSO and ADMM) to evaluate a solution's quality. Its function is to help us find the best solution that minimizes overall costs while ensuring that the system's energy is properly balanced. The optimization problem is expressed using the NBT.

$$\max \ \Pi_{i=1}^{N}(\hat{C}_i - C_i)^{\mathrm{MP}_i} \tag{35}$$

Objective function:

$$\sum \rho w \sum_t \left[\sum_i C_{i,t,w}^{\mathrm{gen}} + \sum_i C_{i,t,w}^{\mathrm{load}} + \sum_i C_{i,t,w}^{\mathrm{bat}} + \sum_{ij} C_{ij}^{\mathrm{sw}} \cdot (u_{ij,t} - u_{ij,t-1}) - \sum_{i \neq j} \pi_{i,t,w} \cdot P_{ij,t,w} \right] \tag{36}$$

The peer-to-peer energy trading problem is expressed using the Nash bargaining theory to ensure fair allocation of costs among microgrids. Although the formulation is compatible with distributed solution techniques such as ADMM and ATC, this study employs PSO as the main optimization engine to solve the integrated problem in a centralized simulation framework. The reference to ADMM/ATC reflects the potential for decentralized implementation rather than an additional solution layer.

2.2 Proposed model

The abovementioned market-clearing problem is inherently nonlinear and mixed-integer due to network constraints and reconfiguration decisions. In this study, PSO is employed as the primary solution method to solve the integrated problem using TPC system data. While the formulation is compatible with distributed solution techniques such as the ADMM, PSO is adopted for centralized simulation to ensure computational tractability and reproducibility. In a distributed implementation, ADMM iterations would decompose the problem across microgrids with local subproblems and coordination variables, terminated when primal and dual residuals satisfy predefined tolerance thresholds. This study adopts a simulation-driven approach to evaluate the integration and dynamic restructuring of hybrid renewable energy units within the TPC distribution framework (Y. Wang et al., 2020). PSO optimization algorithm (Perez-Flores et al., 2021a, Y. Zhang et al., 2015) is employed to coordinate peer-to-peer (P2P) energy trading Click or tap here to enter text.(Z. Wang et al., 2020), while accommodating the intermittent nature of PV and WT resources (De and Mandal, 2022; Deng and Lv, 2020; Konneh et al., 2019). Figure 1 illustrates the overall workflow. The following key assumptions are adopted to ensure computational tractability and consistency of the simulation framework. All electrical loads are modeled as balanced, three-phase equivalent static loads with constant power characteristics over each scheduling interval. The load and renewable generation profiles are assumed to be known within the 24-hour horizon and updated at hourly resolution. Power balance is enforced at every bus, ensuring that total generation, storage dispatch, and P2P energy exchanges exactly match local demand and network losses. The distribution network is assumed to operate under quasi-steady-state conditions, where dynamic transients are neglected and steady-state analysis is used to evaluate power flow constraints. The voltage magnitude and line current limits are strictly enforced to guarantee a feasible and secure operation in all simulated scenarios.

2.2.1 Case Data: IEEE 84-Bus TPC Network

The TPC distribution system provides a comprehensive test environment for reconfiguration analysis under decentralized trading. Its IEEE 84-bus representation captures detailed feeder layouts, switching nodes, and reconfiguration opportunities (Chuang et al., 2019; Liou, 2010). A novel presentation for the IEEE 84-bus topological layout of the TPC represents the following: the points that can be critically used for network reconfiguration, the transmission/distribution line infrastructure, and switching elements. The IEEE 84-bus topology will be the core for our analysis, providing reliable information for assessing the MG reconfiguration optimization algorithms and decentralized P2P energy trading (Sadeghi et al., 2024; Soto et al., 2021; C. Zhang et al., 2021). The benchmark includes the following: (1) Switch status and detailed operational information of switches numbered 1 through 58 (Table 1), (2) Electrical characteristics of feeders such as resistance/reactance (Table 2), and (3) Initial injection parameters for load and generation nodes, enabling computation of secondary parameters and optimized power flow. Line impedance is crucial for optimizing and quantifying energy losses. Tables 3 and 4 show comprehensive tabulations of input power parameters and impedance characteristics, respectively. Table 4 provides a structured compendium of identified open-circuit pathways, offering an overview of network connectivity and electrical properties. This comprehensive dataset is fundamental for accurate power flow calculations and network analysis. Table 3 shows the inventories of potential network reconfiguration pathways based on the current open state of specific switching devices. These latent topological alternatives, defined by line paths and critical open switches, underscore the inherent design flexibility of the distribution network. They serve as crucial assets for advanced power system strategies, including load balancing, fault isolation, and alternative supply routes, facilitating deliberate modification of power flow patterns and enhancing network resilience.

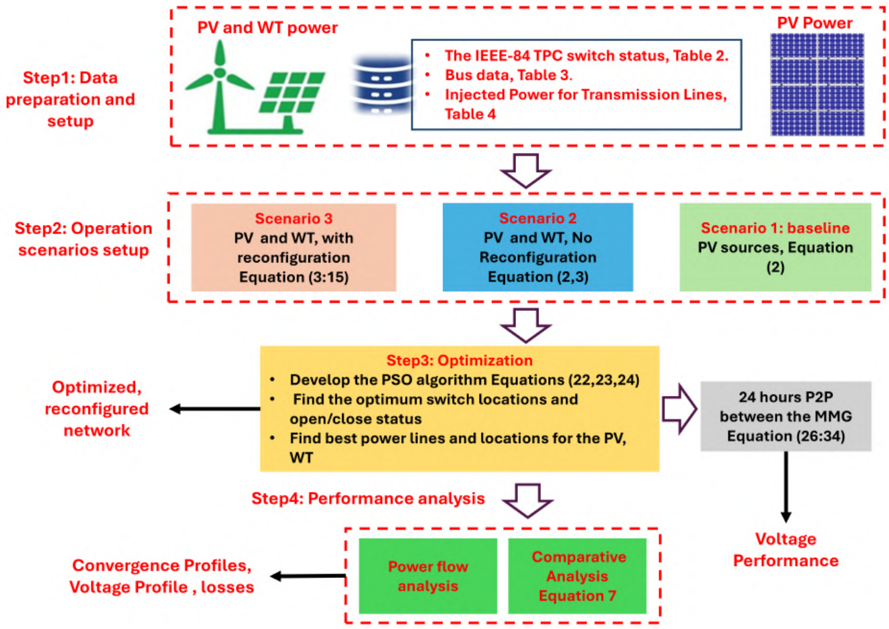

Figure 1 Workflow of the proposed PV–WT integration and adaptive reconfiguration strategy for the thermoplastic cell system

2.2.2 PSO model for network optimization

This section details the sequential application of the PSO algorithm, conceptually depicted in Figure 2, across distinct stages to achieve optimal system configuration and operational parameters. The overarching objective is to minimize power costs and reduce losses within the network, considering various RES integration scenarios (Parvin et al., 2023). The process begins with a careful definition of decision variables, search intervals, and a cost function benchmarked against the IEEE 84-bus system. Algorithm-specific hyperparameters, such as swarm size, maximum generations, inertia factor with damping, and learning constants, are tuned to maintain the balance between exploration and exploitation (Perez-Flores et al., 2021b). Each particle is randomly initialized and iteratively updated according to its own best record and the global best of the swarm. The search converges toward an optimal configuration that specifies switch states, injection levels, and power flow solutions with inertia weight decaying over time. These outputs form the basis for improved reconfiguration strategies. The number of particles and iterations in the PSO algorithm were selected based on a trade-off between convergence reliability and computational efficiency. A swarm size of 10 agents was sufficient to ensure adequate exploration of the solution space, given the moderate dimensionality of the optimization problem and the decision variables' structured nature.

Table 1 Status of Switches in the IEEE 84-Bus Distribution Network Under Normal Operating Conditions

Conditions								
Switch Number	**Status**	**Connecting Buses**	**Switch Number**	**Status**	**Connecting Buses**	**Switch Number**	**Status**	**Connecting Buses**
1	Closed	connection near S1	33	Closed	32–33	65	Closed	connection near S2
2	Closed	1–2	34	Closed	33–34	66	Closed	65–66
3	Closed	2–3	35	Closed	34–35	67	Closed	66–67
4	Closed	3–4	36	Closed	35–36	68	Closed	67–68
5	Closed	4–5	37	Closed	36–37	69	Closed	68–69
6	Closed	5–6	38	Closed	37–38	70	Closed	69–70
7	Closed	6–7	39	Closed	38–39	71	Closed	70–71
8	Open	Branching	40	Closed	39–40	72	Closed	71–72
9	Closed	Branching from 8–9	41	Closed	40–41	73	Closed	connection near S2
10	Open	9–10	42	Closed	41–42	74	Closed	73–74
11	Closed	connection near S1	43	Closed	42–43	75	Closed	74–75
12	Closed	11–12	44	Closed	43–44	76	Closed	75–76
13	Open	12–Branching	45	Closed	44–45	77	Closed	76–77
14	Open	Branching from 13	46	Closed	45–46	78	Closed	77–78
15	Closed	connection near S1	47	Closed	near S2	79	Closed	78–79
16	Closed	15–16	48	Closed	47–48	80	Closed	79–80
17	Closed	16–17	49	Closed	48–49	81	Closed	80–81
18	Closed	17–18	50	Closed	49–50	82	Closed	81–82
19	Closed	18–19	51	Closed	50–51	83	Closed	82–83
20	Closed	19–20	52	Closed	51–52	84	Open	Multiple branching
21	Closed	20–21	53	Closed	52–53	85	Open	Reconfiguration
22	Open	21–Branching	54	Closed	53–54	86	Open	Reconfiguration
23	Closed	Branch from 22–23	55	Closed	54–55	87	Open	Reconfiguration
24	Closed	23–24	56	Closed	near S2	88	Open	Reconfiguration
25	Closed	connection near S1	57	Closed	56–57	89	Open	Reconfiguration
26	Closed	25–26	58	Closed	57–58	90	Open	Reconfiguration
27	Closed	26–27	59	Closed	58–59	91	Open	Reconfiguration
28	Closed	27–28	60	Closed	59–60	92	Open	Reconfiguration
29	Closed	28–29	61	Closed	60–61	93	Open	Reconfiguration
30	Closed	connection near S1	62	Closed	61–62	94	Open	Reconfiguration
31	Closed	30–31	63	Closed	62–63	95	Open	Reconfiguration
32	Closed	31–32	64	Closed	63–64	96	Open	Reconfiguration

Increasing the swarm size beyond this value did not yield noticeable improvements in the solution quality while significantly increasing the computational burden. Similarly, 200 iterations were selected to guarantee stable convergence of the objective function, as preliminary convergence tests showed that the algorithm consistently reached near-optimal solutions well before the maximum iteration limit. This configuration ensures robust convergence while maintaining a reasonable simulation time. The active and reactive power demands at each bus were adopted from the IEEE 84-bus TPC distribution test system. All loads are modeled as constant PQ loads. A normalized 24-hour load profile is applied to represent daily demand variation, with peak demand occurring during the evening hours.

The same temporal profile is used for all buses, whereas individual bus loads are scaled according to their nominal P/Q ratings. Photovoltaic generation is modeled based on a typical daily solar irradiance profile, with peak irradiance at midday and zero output during the night. The wind turbine generation follows a standard wind speed profile with moderate temporal variability. We incorporate renewable uncertainty by modeling actual generation as a nominal forecast plus a stochastic deviation. The deviation is assumed to follow a zero-mean distribution, and its variance is used in the objective function to penalize volatile operating solutions.

Table 2 Electrical Characteristics of TPC Distribution Network Transmission Lines

Buses						**Buses**						**Buses**					
from	to	R(Ω)	X(Ω)	$\frac{B}{2}$	A	from	to	R(Ω)	X(Ω)	$\frac{B}{2}$	A	From	To	R(Ω)	X(Ω)	$\frac{B}{2}$	A
1	2	0.1944	0.6624	0	1	33	34	0.0262	0.0538	0	1	1	6	0.0486	0.1656	0	1
2	3	0.2096	0.4304	0	1	34	35	0.1703	0.3497	0	1	66	67	0.1703	0.3497	0	1
3	4	0.2358	0.4842	0	1	35	36	0.0524	0.1076	0	1	67	68	0.1215	0.4114	0	1
4	5	0.0917	0.1883	0	1	36	37	0.4978	1.0222	0	1	68	69	0.2187	0.7452	0	1
5	6	0.2096	0.4304	0	1	37	38	0.0393	0.0807	0	1	69	70	0.0486	0.1656	0	1
6	7	0.0393	0.0807	0	1	38	39	0.0393	0.0807	0	1	70	71	0.0729	0.2484	0	1
7	8	0.0406	0.1380	0	1	39	40	0.0786	0.1614	0	1	71	72	0.0567	0.1932	0	1
8	9	0.1048	0.2152	0	1	40	41	0.2096	0.4304	0	1	72	73	0.0262	0.0538	0	1
8	10	0.2358	0.4842	0	1	39	42	0.1965	0.4035	0	1	1	74	0.3241	1.1040	0	1
8	11	0.1048	0.2152	0	1	42	43	0.2096	0.4304	0	1	74	75	0.0324	0.1104	0	1
1	12	0.0786	0.1614	0	1	1	44	0.0486	0.1656	0	1	75	76	0.0567	0.1932	0	1
12	13	0.3406	0.6944	0	1	44	45	0.0393	0.0807	0	1	76	77	0.0486	0.1656	0	1
13	14	0.0262	0.0538	0	1	45	46	0.1310	0.2690	0	1	1	78	0.2511	0.8556	0	1
13	15	0.0786	0.1614	0	1	46	47	0.2358	0.4842	0	1	78	79	0.1296	0.4416	0	1
1	16	0.1134	0.3864	0	1	1	48	0.2430	0.8280	0	1	79	80	0.0486	0.1656	0	1
16	17	0.0524	0.1076	0	1	48	49	0.0655	0.1345	0	1	80	81	0.1310	0.2640	0	1
17	18	0.0524	0.1076	0	1	49	50	0.0655	0.1345	0	1	81	82	0.1310	0.2640	0	1
18	19	0.1572	0.3228	0	1	50	51	0.0393	0.0807	0	1	82	83	0.0917	0.1883	0	1
19	20	0.0393	0.0807	0	1	51	52	0.0786	0.1614	0	1	83	84	0.3144	0.6456	0	1
20	21	0.1703	0.3497	0	1	52	53	0.0393	0.0807	0	1	6	56	0.131	0.269	0	1
21	22	0.2358	0.4842	0	1	53	54	0.0786	0.1614	0	1	8	61	0.131	0.269	0	1
22	23	0.1572	0.3228	0	1	54	55	0.0524	0.1076	0	1	12	44	0.131	0.269	0	1
22	24	0.1965	0.4035	0	1	55	56	0.1310	0.2690	0	1	13	73	0.3406	0.6944	0	1
24	25	0.1310	0.2690	0	1	1	57	0.2268	0.7728	0	1	14	77	0.4585	0.9415	0	1
1	26	0.0567	0.1932	0	1	57	58	0.0531	0.1729	0	1	15	19	0.5371	1.0824	0	1
26	27	0.1048	0.2152	0	1	58	59	0.0524	0.1076	0	1	17	27	0.0917	0.1883	0	1
27	28	0.2489	0.5111	0	1	59	60	0.0405	0.1380	0	1	21	84	0.0786	0.1614	0	1
28	29	0.0486	0.1656	0	1	60	61	0.0393	0.0807	0	1	29	33	0.0524	0.1076	0	1
29	30	0.1310	0.2690	0	1	61	62	0.0262	0.0538	0	1	30	40	0.0786	0.1614	0	1
1	31	0.1965	0.3960	0	1	62	63	0.1048	0.2152	0	1	35	47	0.0262	0.0538	0	1
31	32	0.1310	0.2690	0	1	63	64	0.2358	0.4842	0	1	41	43	0.1965	0.4035	0	1
32	33	0.1310	0.2690	0	1	64	65	0.0243	0.0828	0	1	54	65	0.0393	0.0807	0	1

Table 3 Initial Injected Power for Transmission Lines. This table presents the initial power injected into each transmission line

Power index	Line Injection power (MW)	Power index	Line Injection power (MW)
1	488.712139517526	13	1200
2	1200	14	0
3	1200	15	1166.23993372747
4	117.344788762350	16	1200
5	122.066192223495	17	1200
6	1019.65073498411	18	1200
7	1124.81406364160	19	1200
8	777.261295231962	20	1200
9	1184.07666584809	21	1200
10	140.748290651205	22	1200
11	1200	23	0
12	1035.28296513910	24	1200

Table 4 Potential network reconfiguration paths, identified by open switches and bus sequences, offering operational flexibility

Line path	Description
[86 11]	Open switch 86 at bus 11 indicates a potential network reconfiguration point or inactive branch near substation S1.
[89 14]	Open switch 89 at bus 14 suggests an alternative connection for load balancing or fault isolation in the central-left network.
[90 15 16]	Open switch 90 across buses 15 and 16 signifies a potential bypass or alternative route in the lower-left network, near substation S1.
[92 27 28]	Open switch 92 at buses 27 and 28 suggests a possible alternative feeder or connection in the central-left network.
[93 29 39]	Open switch 93 connecting buses 29 and 39 indicates a potential tie-line or alternative supply route between central-left and lower-middle network sections.
[94 33 34]	Open switch 94 at buses 33 and 34 suggests an alternative connection for operational flexibility in the lower middle network.
[95 40 41 42]	Open switch 95 across buses 40, 41, and 42 indicates a potential network extension or alternative connection at the lower network edge.
[84 53 54 55]	Open switch 84 at buses 53, 54, and 55 suggests an alternative feeder or connection in the upper-right network, potentially branching from the S2 supply.
[96 62 63 64]	Open switch 96 across buses 62, 63, and 64 indicates a potential bypass or alternative route in the upper-right network.
[87 67 68 69 70 71 72]	Open switch 87 across buses 67–72 in the central-right section suggests a potential tie-line or alternative supply route connecting different feeders.
[88 74 75 76]	Open switch 88 across buses 74, 75, and 76 indicates a potential bypass or alternative route in the lower-right network.
[91 80 81 82 83]	Open switch 91 across buses 80–83 in the lower-right section suggests a potential tie-line or alternative supply route connecting different feeders.
[84 55 64]	Open switch 85 connecting buses 55 and 64 potentially indicates a tie-line linking the S2-fed upper-right section to another network part.

The line thermal limits are defined based on the maximum allowable current ratings derived from the line parameters. The bus voltage magnitudes are constrained within ±5% of the nominal values. Switch operations are limited to the predefined sectionalizing and tie switches listed in Table X, ensuring a radial network topology throughout all reconfiguration scenarios.

2.2.3 Multi-operation scenarios

Multiple case studies were designed to evaluate the methodology, focusing on the uncertainty of renewable generation and its implications for P2P trading dynamics among MGs (Ahmed et al., 2024; Elkadeem et al., 2019). The analysis begins with a baseline evaluation of the TPC network's integration of PV generation with PSO-based optimal switch allocation to address cost uncertainty and voltage drop. Then, it expands to incorporate both WT and PV generation, again using PSO for optimal switch locations (still without reconfiguration). A pivotal stage introduces network reconfiguration along with PSO to optimize switch locations and states for combined PV/WT integration to minimize losses and achieve optimal cost (Nguyen and Nguyen, 2025). Finally, the analysis culminates in an investigation of 24-hour energy trading dynamics under full PV/WT capacity, comparing scenarios with and without network reconfiguration to explicitly demonstrate its impact on P2P trading efficiency and effectiveness. A Monte Carlo scenario-based approach is used to model renewable generation uncertainty. A total of N_s scenarios are generated by adding stochastic forecast errors to the nominal PV irradiance and wind speed profiles. The forecast errors are assumed to follow a zero-mean normal distribution with predefined variance, consistent with the objective function's variance-based penalty term. All scenarios are evaluated over the 24-hour scheduling horizon, and the expected values and confidence intervals of key performance metrics are computed. The reported results correspond to the mean values across all scenarios, with 95% confidence intervals computed for power loss, operational cost, and voltage deviation. To assess robustness, the weighting factor w was varied within the range $[0.3, 0.7]$. The results indicate that while the absolute cost and resilience values change with w, the relative performance ranking of different configurations remains consistent. Sensitivity analysis was performed with respect to the PSO parameters, including the swarm size and maximum iteration count. The algorithm consistently converged to near-optimal solutions with marginal performance variation, indicating low parameter tuning sensitivity. Additional simulations conducted by varying the total installed PV and WT capacities from 20% to 60% of the peak load. The results confirm that the proposed framework is feasible and stable across different renewable penetration levels. All simulations and optimization procedures were performed using MATLAB. The PSO algorithm and power flow calculations were developed in the MATLAB environment, enabling flexible handling of nonlinear constraints, switch-based network reconfiguration, and peer-to-peer (P2P) energy trading mechanisms. Using customized scripts, steady-state power flow analysis was performed to evaluate voltage profiles, line currents, and system losses under different operating scenarios.

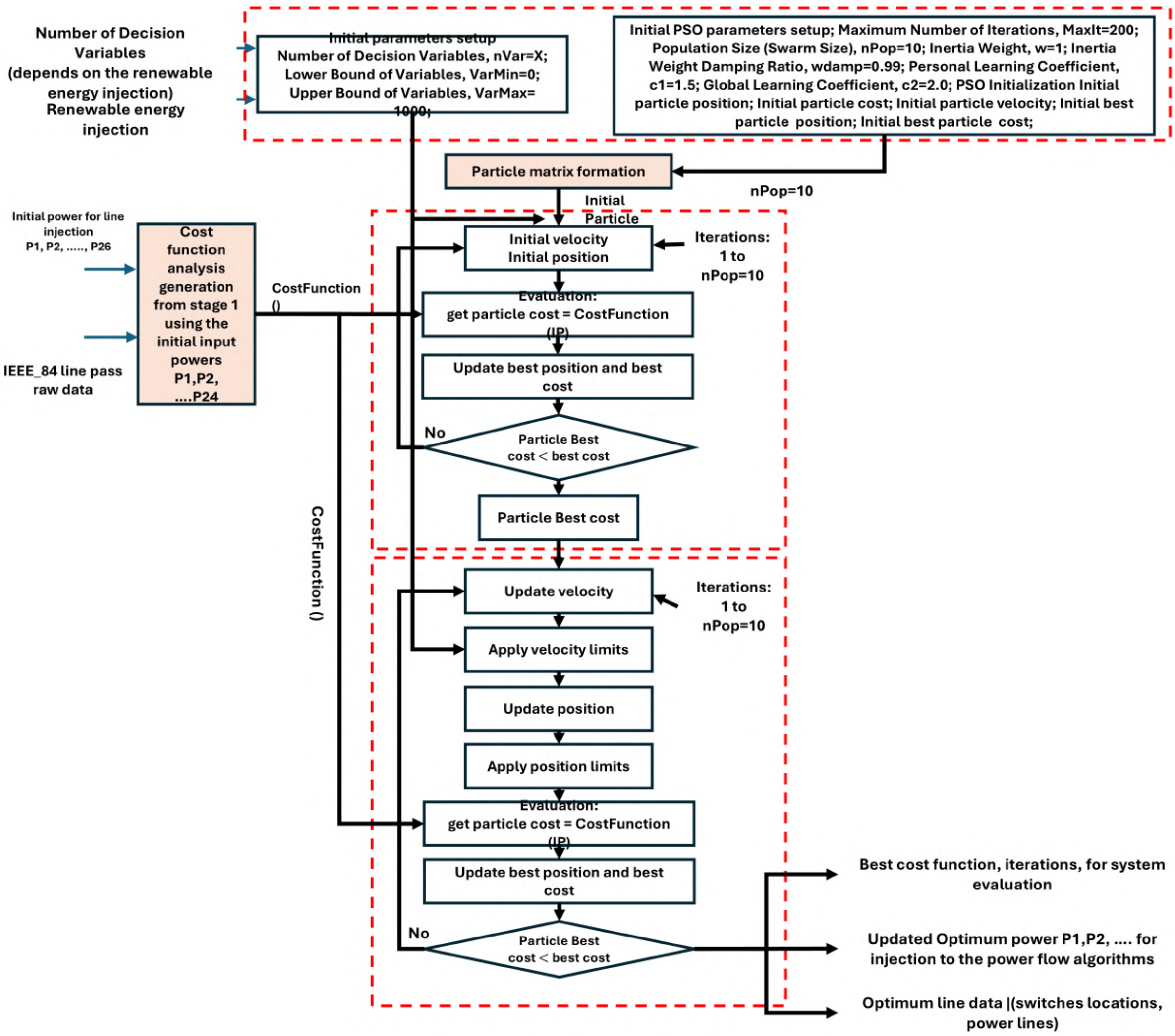

Figure 2 Detailed flowchart of the PSO algorithm for distribution system optimization and network configuration

3. Result and Discussion

3.1 Scenario 1

The first case investigates the system operation under PV integration. The PSO algorithm is used to determine network settings that minimize losses and operating expenses. The analysis includes identification of the best PV locations, partitioning into local microgrids, evaluation of system losses, convergence of the optimization, and improvements in voltage stability.

3.1.1 Optimal PV placement and microgrid structure

As shown in Figure 3, the IEEE 84-bus network is divided into two microgrids. Within these structures, PV installations are strategically placed at optimal bus locations, identified through the PSO algorithm: MG1 includes PVs at Buses 10, 12, 15, 18, 27, 34, 43, and 46, while MG2 integrates units at Buses 51, 59, 71, and 78. These placements are critical for maximizing the benefits of renewable energy, improving local voltage profiles, and reducing overall system losses.

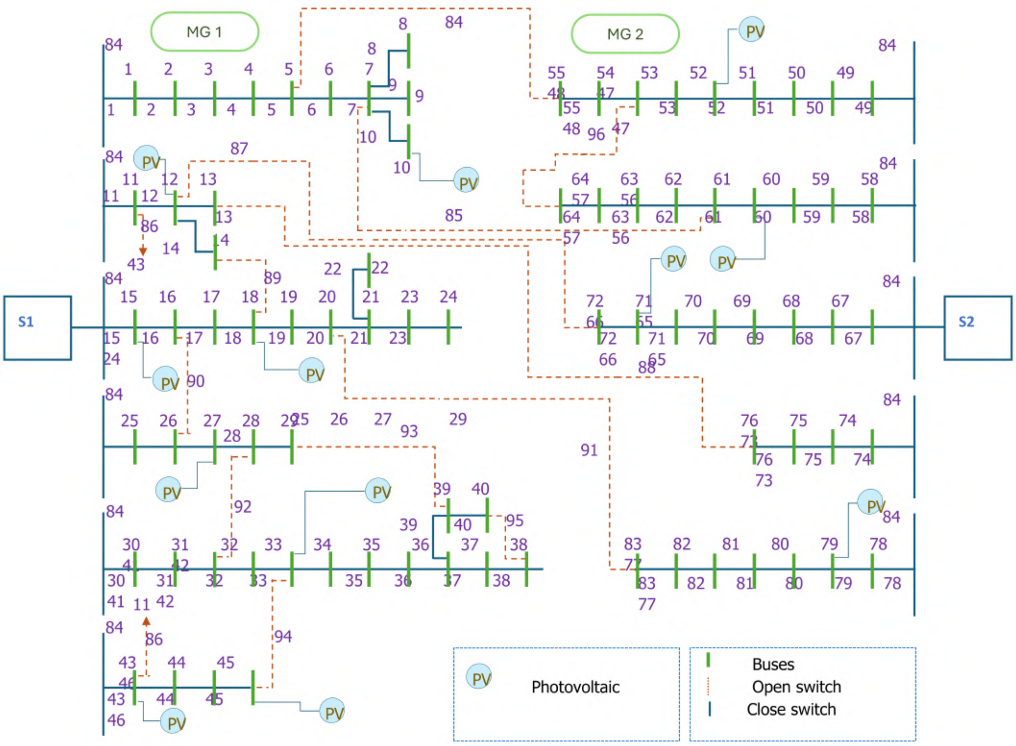

Figure 3 Topological representation of the TPC distribution network with integrated PV MGs

3.1.2 Performance analysis (power loss, cost optimization, and voltage profile)

Strategic PV integration within the TPC network resulted in substantial reductions in power losses and operational costs, especially during the simulated 24-hour energy trading period. The 200-iteration PSO optimization, conceptually illustrated by the network configuration, converged from an initial best cost of 5.0 USD/MWh to approximately 2.3729 USD/MWh by the 200th iteration, demonstrating the scheme's effectiveness in optimizing energy delivery and minimizing financial costs. Concurrently, PV integration with PSO profoundly improved the network voltage stability (Figure 4), yielding a remarkably stable voltage profile across the entire system.

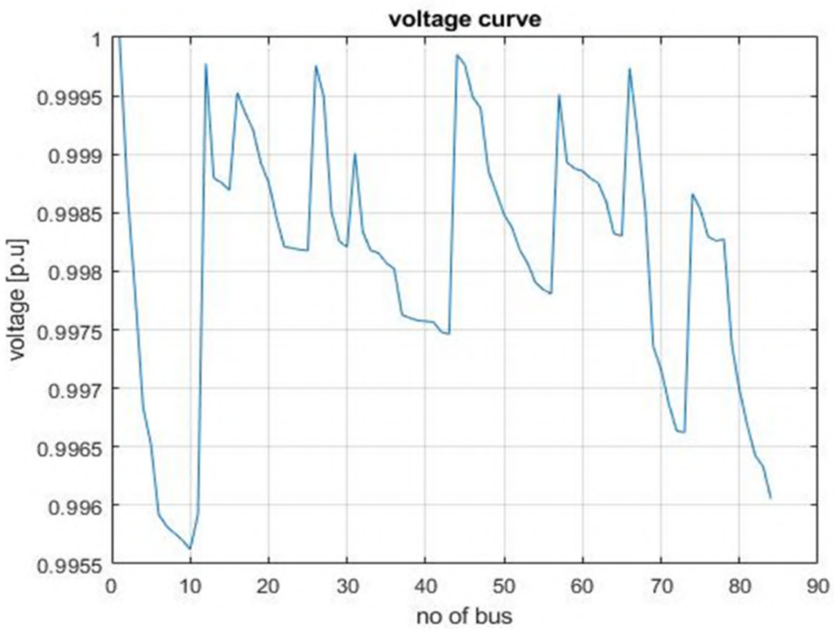

Figure 4 Bus voltage magnitudes for the PV optimized TPC configuration

Quantitatively, after optimized PV integration, the active power losses dramatically decreased from 4.924 MW to an impressively low 0.0024 MW signifying an extraordinary enhancement in energy efficiency.

3.2 Scenario 2

The second case study investigates the TPC network under the simultaneous deployment of PV and wind resources. The optimization problem becomes more complex when two inherently variable energy sources operate in tandem. The PSO algorithm is employed to navigate this high-dimensional search space, continuously refining dispatch strategies and ensuring stable system operation despite variability. Subsequent analysis details the system's performance under this hybrid integration.

3.2.1 Optimal placement of the PV and WT

Figure 5 visually delineates the MG and initial PV and WT integrations. In this hybrid scenario, the PSO algorithm is leveraged to identify the most advantageous bus locations for all renewable energy sources. Thus, this precise and optimized allocation of both PV and WT units is a critical enabler for the efficient and reliable operation of the TPC network under diversified renewable energy's high penetration.

3.2.2 Power loss, cost optimization, and voltage profile

As shown in Figure 6, starting at 9.0 USD/MWh, the operational cost rapidly fell to approximately 5.0 USD/MWh within the first iteration and eventually stabilized at 2.1011 USD/MWh after approximately 140 iterations. This highlights the capability of PSO to handle the larger decision space created by integrating two intermittent sources. From a technical perspective, the active power losses were reduced to 0.0021 MW, improving upon the PV-only result of 0.0024 MW and representing a dramatic improvement relative to the baseline value of 4.924 MW. Voltage magnitudes across buses also became smoother and more robust, ensuring system reliability even under fluctuating renewable output. Overall, the hybrid PV–WT deployment clearly outperforms single-source integration, yielding a more efficient, stable, and environmentally aligned distribution system.

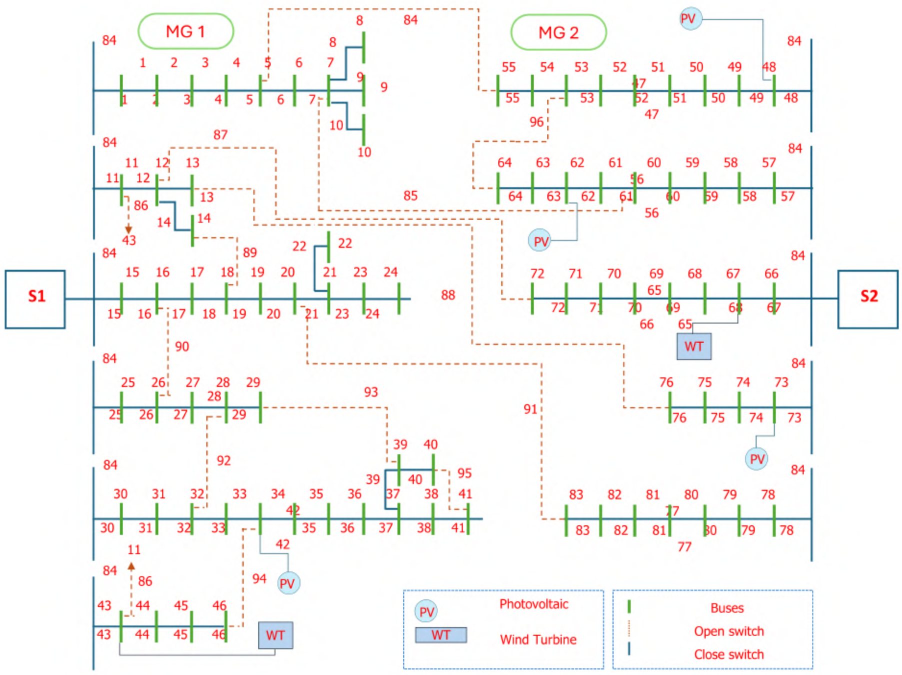

Figure 5 Optimized hybrid PV-WT deployment across the IEEE 84-bus TPC network for Scenario 2 with MG1 and MG2

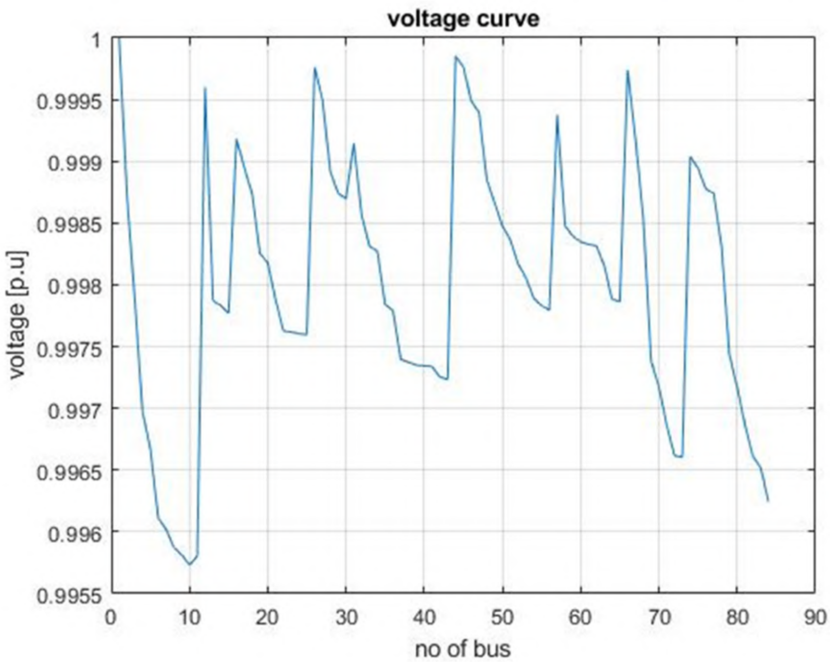

Figure 6 Voltage profile for the hybrid renewable integration of the TPC

3.3 Scenario 3

The third scenario introduces dynamic grid reconfiguration along with renewable integration to push system performance beyond that of the PV-only and hybrid scenarios. The evaluation emphasizes how reconfiguration reshapes the network layout, lowers losses, reduces operating costs, and strengthens voltage stability.

3.3.1 Network reconfiguration scheme and topology

The resulting optimized network topology, visually illustrating altered switch states and delineating MG1 and MG2, is presented in Figure 7. The application of this coordinated reconfiguration, alongside continued PV and WT integration, yielded further significant reductions in energy losses and operational costs.

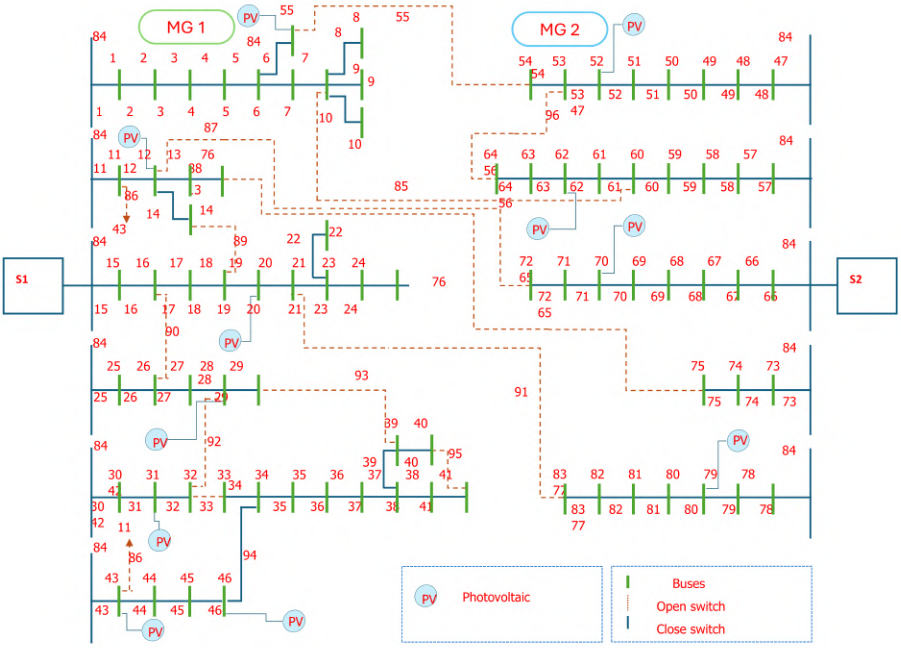

Figure 7 Topology optimization of the IEEE 84-bus network under coordinated reconfiguration

3.3.2 Power loss, cost optimization, and voltage profile

As shown in Figure 8, the optimization process, commenced with an initial best cost of 8.0 \$/MWh, rapidly decreased to 5.2 \$/MWh, and stabilized at a remarkably low 1.954 \$/MWh by iteration 120, demonstrating superior economic performance. A direct comparison with scenario 2 reveals that the total power losses were reduced from 0.0021 MW to 0.002 MW, and the best cost was improved from 2.1011 \$/MWh to 1.954 \$/MWh. Compared to the baseline system (Scenario 1), power losses drastically reduced from 0.0024 MW to an exceptional 0.002 MW, unequivocally showcasing dramatic improvements in energy efficiency and cost-effectiveness. Enhanced voltage stability is evident in the voltage profile across system buses, demonstrating highly minimal fluctuations.

3.4 P2P trading in energy

When energy trading is conducted without network reconfiguration, the system experiences several significant drawbacks. First, voltage levels are subject to sharp fluctuations, frequently dropping below 0.975 p.u., particularly during periods of high trading activity. Second, such conditions lead to increased power losses, which are primarily attributable to suboptimal power distribution pathways and the inefficient utilization of available renewable energy sources. Consequently, the operational costs of energy supply remain high, driven by unnecessary energy dissipation and congestion within transmission lines. Conversely, the dynamic adjustment of switching states, facilitated by network reconfiguration, is instrumental in establishing a more balanced and efficient energy distribution framework. This strategic approach yields substantial improvements across key performance metrics. First, the system exhibited significantly enhanced voltage stability consistently maintaining voltage levels around 0.99 p.u. throughout the entire day. Second, network reconfiguration leads to a substantial reduction in power losses by optimizing the energy flow between microgrids. Finally, the overall expense associated with energy trading is considerably lowered, as reconfiguration mitigates the need for additional energy generation and other compensating measures that would otherwise be necessary to address inefficiencies. Figure 9 shows the comparative voltage performance for both scenarios (with and without reconfiguration) across each hour of the day.

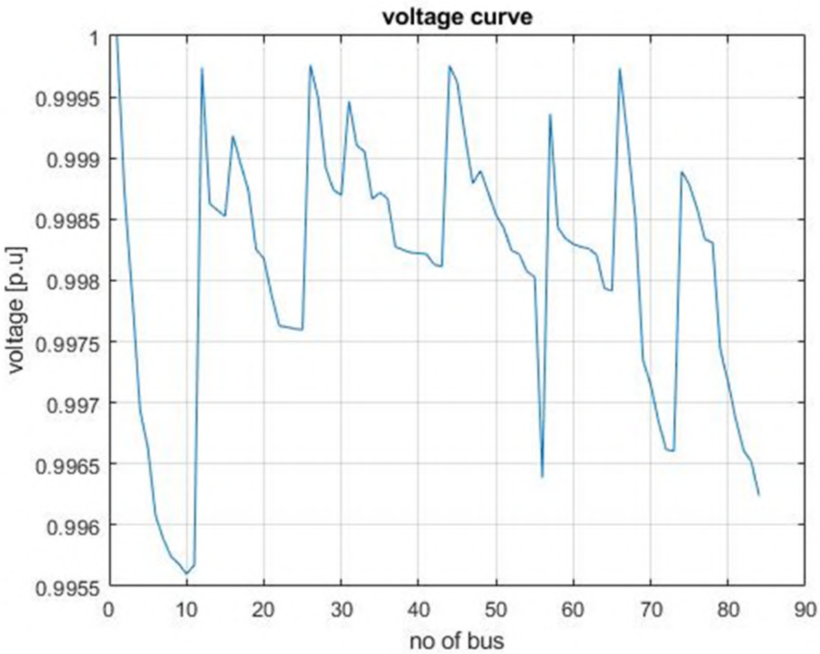

Figure 8 Voltage profile of the TPC under optimized PV and WT integration with network reconfiguration

All comparative scenarios use identical PV/WT capacities and P2P trading parameters; the only difference is the network reconfiguration activation. PSO is compared against a GA-based reconfiguration method commonly adopted in distribution network studies for benchmarking purposes. Both algorithms use the same objective function, constraints, and stopping criteria, and their computational performance is compared in Table 5.

Table 5 Comparison of computational performance

Method	Iteration	CPU time (s)
GA	200	145
PSO	200	62

A benchmarking analysis was conducted to assess the effectiveness of the proposed PSO-based framework. First, the system performance with and without network reconfiguration was compared under identical renewable generation and P2P trading assumptions. This comparison isolates the impact of reconfiguration on losses, voltage stability, and operational cost. In addition, PSO was benchmarked against a representative heuristic optimization method commonly used in DNR. Both methods used the same objective function, constraints, and termination criteria. The convergence behavior and computational time were evaluated to assess scalability. The results indicate that PSO converges faster and achieves superior or comparable solutions with lower computational burden, making it suitable for large-scale, network-constrained P2P energy trading problems.

4. Conclusions

This study presents a comprehensive comparative analysis of various power distribution network configurations, highlighting the significant benefits of integrating renewable energy systems with flexible grid configurations. The primary goal of this study was to optimize energy trading within the power distribution network. The results consistently demonstrate that this advanced configuration delivers excellent performance across key aspects, including voltage stability, reduced power loss, and overall cost reduction. A key finding of our comparative analysis is the significant improvement in voltage stability achieved through network reconfiguration, particularly during continuous 24-hour power trading. The multi-stage optimization process consistently showed that energy trading augmented with network reconfiguration is the most optimal methodology. This configuration yielded the best results in terms of cost-effectiveness, substantial power loss reduction, and superior voltage regulation. The final optimized scenario achieved the lowest recorded operational cost of $1.954/MWh and remarkably reduced total active power losses to 0.002 MW. These figures represent a drastic improvement compared to the initial baseline (Scenario 1) system (PV integration with network optimization), where power losses were as high as 0.0024 MWh and operational costs were significantly greater (2.3729 $/MW). Through a comparative study of three distinct system configurations, we observed a clear progression of performance enhancements: normal operation with PV only (Scenario 1), normal operation with PV and WT (Scenario 2), and Reconfigured System with PV and WT injection (Scenario 3). The PV and WT with Reconfiguration demonstrated the fastest convergence rate and culminated in the lowest operational cost, proving to be the most efficient and optimal solution. Figure 10 illustrates the convergence behavior of the PSO algorithm for the three system configurations investigated: PV-only integration, combined PV and wind integration, and PV–wind integration with network reconfiguration. As shown, all cases exhibit a monotonic decrease in the objective function value, confirming the optimization process's stable convergence. However, the reconfigured PV–wind system demonstrates a significantly faster convergence rate and the lowest final cost. This improved performance is attributed to the additional flexibility introduced by network reconfiguration, which enlarges the feasible search space and enables more effective loss minimization and power flow redistribution. In contrast, the PV-only case converges more slowly and stabilizes at a higher cost level, indicating limited optimization flexibility when reconfiguration and wind generation are not considered.

Further detailed performance evaluations of these configurations, including best cost and total power losses, are systematically presented in Table 6 and Figure 11 and Figure 12. This table confirms the reconfiguration approach's superiority, as it consistently provided the minimum best operational cost of $1.954/MWh and achieved the lowest total power losses of 0.0020 MW.

Table 6 Evaluation of the Comparative Performance of Key Optimal Metrics for Different System Configurations

Parameter	System with PV Only (Scenario 1)	System with PV and WT (Scenario 2)	System with PV and WT with Reconfiguration (Scenario 3)
Best Cost ($/MWh)	2.3729	2.1011	1.954
Total power loss (MW)	0.0024	0.0021	0.0020
Number of Search Agents (A)	10	10	10
Iterations	200	200	200

The observed reduction in power losses and operational costs translates into tangible benefits for distribution system operators and prosumers. Lower network power losses directly reduce unnecessary energy dissipation, leading to improved system efficiency, reduced thermal stress on distribution lines, and extended equipment lifespan. From an economic perspective, the operational cost reduction reflects decreased reliance on upstream energy procurement and more efficient use of locally generated renewable energy through P2P trading. These savings can be passed on to end-users as lower electricity tariffs or reinvested in grid modernization and renewable expansion. Moreover, improved loss performance enhances voltage regulation and network reliability, facilitating higher penetration of distributed energy resources without violating operational constraints. Ultimately, this research firmly establishes that the synergistic combination of optimally placed hybrid PV and wind generation with dynamic network reconfiguration is the most effective strategy for enhancing modern distribution networks' efficiency, reliability, and economic viability. Network reconfiguration is an indispensable tool for achieving optimum cost and loss reduction in energy distribution, particularly for facilitating stable and sustainable peer-to-peer energy trading operations within evolving smart grid paradigms.

Table 7 Summary of Relevant Literature, Research Gaps, and Contribution of This Research

Study	System Scope	Methods Used	Cost Reduction	Power loss reduction	P2P Trading	Reconfiguration	Uncertainty Handling
Albadi and El-Saadany, 2008	Market-level	Demand Response	5–15%	—	×	×	×
Chen et al., 2021	Single MG	Stochastic Optimization	8.5%	—	×	×	✓
Lv and Ai, 2016	Networked MGs	Interactive Optimization	9.3%	—	×	×	Partial
Thakar et al., 2019	Microgrid	Reconfiguration	—	12–18%	×	✓	×
Keck et al., 2019	National Grid	Battery Integration	Curtailment ↓ 81%	—	×	×	×
Nazemi et al., 2021	Resilient MG	MESS + Reconfiguration	—	—	×	✓	✓
Zare et al., 2024	Multi-MG	Hybrid Stochastic-Robust	11.3–13.2%	—	×	✓	✓
T. Wang et al., 2025	MG	Uncertainty-Aware DDPG	14.8%	—	×	×	✓
This work (proposed model)	TPC IEEE-84 Bus	PSO + Reconfiguration + P2P	17.7% ↓ (2.3729 → 1.954 $/MWh)	≈ 99.96% ↓ (4.924 → 0.002)	✓	✓	✓

Author Contributions

Ghaith M. Fadhil: Conceptualization, Methodology development, Software implementation, Formal analysis, Investigation, and Writing – original draft preparation. Saeid Ghassem Zadeh: Supervision, Validation, Critical review, and Writing – review & editing. Sina Roudnil: Data curation, Visualization, Resource provision, and Writing – review & editing.

Conflict of Interest

"The authors declare no conflicts of interest."

Supplementary Materials

Supplementary File 4: Figures and tables

List of signs and symbols

Symbol	Description	Symbol	Description
$C_i(x_i)$	Cost function for each microgrid or participant	p	Air density
λ	Weight factor for uncertainty variance penalty	v	Wind speed
$\mathrm{Var}(\Delta P_{RE})$	Variance of the uncertainty in renewable energy	C_p	Turbine power factor
η_{PV}	Efficiency of the PV module	$P_{k,t}^{\mathrm{net}}$	Represent the power flow in the reconfigurable network.
A	Area of the PV module	$P_{ik,t}$	Active power flow from node i to node k at time t.
G	Solar irradiance (W/m^2)	$Y_{ik,t}$	A binary variable (0 or 1) related to the status of the connection or line between node i and node k at time t.
θ	Angle of incidence of sunlight on the panel	$Q_{k,t}^{\mathrm{net}}$	Net reactive power at node k at time t.
$U_{k,t}$	Voltage magnitude at bus k at time t	$Q_{ik,t}$	Reactive power flow from node i to node k at time t.
$U_{i,t}$	Voltage magnitude at bus i at time t	x_{ik}	Reactance of the line/branch connecting bus i to bus k. This is also typically a fixed parameter of the line.
r_{ik}	Resistance of the line/branch connecting bus i to bus k. This is typically a fixed parameter of the line.	$U_i^{\min}$	Minimum permissible voltage magnitude at bus i.
$C_{i,t}^{\mathrm{Gen}}$	Total generation cost for component i at time t	$U_i^{\max}$	Maximum permissible voltage magnitude at bus i.
λ_i^{MT}	Cost coefficient (or price) for electricity generated by a specific type of generator MT	$H_{i,t}^{\mathrm{TSC}}$	Capacity or amount related to "TS"
λ_i^{BS}	Cost coefficient (or price) for buying/selling electricity from a specific "BS" source	k_i^{TS}	Cost coefficient (or penalty) related to "TS"
$H_{i,t}^{\mathrm{TSD}}$	Demand or discharge related to "TS"	$H_{i,t}^{\mathrm{Ref}}$	Net thermal load of node i at time t
$P_{i,t}^{\mathrm{Ref}}$	Net electrical load of node i at time t	$P_{i,t}^{\mathrm{D}}$	Electrical demand
$H_{i,t}^{\mathrm{D}}$	Thermal demand	$P_{i,t}^{\mathrm{MT}}$	Power generated by microturbines
$H_{i,t}^{\mathrm{MT}}$	Thermal power generated by microturbines	$P_{i,t}^{\mathrm{RES}}$	Renewable energy generation
$P_{i,t}^{\mathrm{BSC}}$	Battery storage charging	$P_{i,t}^{\mathrm{BSD}}$	Battery storage discharging
$H_{i,t}^{\mathrm{TSC}}$	Thermal storage charging	$H_{i,t}^{\mathrm{TSD}}$	Thermal storage discharging
$P_{i,s,t}^{\mathrm{mt}}$	Power generated by microturbines	$P_{i,t}^{\mathrm{dis}}$	Power discharged from battery storage
$P_{i,s,t}^{\mathrm{w}}$	Wind power generation	$P_{i,s,t}^{\mathrm{ms}}$	Total energy traded with other microgrids
$P_{i,t}^{\mathrm{load}}$	Load demand	$P_{i,s,t}^{\mathrm{sh}}$	Power charged into battery storage
C^{ls}	Network loss cost	$P_{i,t}^{\mathrm{MT}}$	Power generated by microturbines
C_i^{sw}	Switching cost	$P_{i,t}^{\mathrm{RES}}$	Renewable energy generation
C^{its}	Wheeling fees	$P_{i,t}^{\mathrm{BSC}}$	Battery storage charging

List of signs and symbols – *(Continued from previous page)*			
Symbol	Description	Symbol	Description
$P_{i,t}^{\mathrm{BSD}}$	Battery storage discharging	$e_{ij,t}^{\mathrm{DN}}$	Energy transferred from microgrid i to microgrid j at time t
$e_{ij,t}^{\mathrm{DN}}$	Energy transferred from microgrid j to microgrid i at time t	MP_i	Market power of agent i
$\tilde{C}_i$	Cost without P2P trading	C_i	Cost with P2P trading
ρ_i	Risk weight	ξ_i	Value at risk
$\delta_{i,s}$	Difference between actual cost and value at risk	$C_{i,t}^{Gen}$	Generation cost
$C_{i,t}^{\mathrm{Bill}}$	Utility bill	$C_{i,t}^{\mathrm{Disc}}$	Discomfort cost
$C_{i,t}^{\mathrm{P2P}}$	P2P trading cost		

References

Ahmed, Mirsaeidi, S., Koondhar, M. A., Karami, N., Tag-eldin, E. M., Ghamry, N. A., El-Sehiemy, R. A., Alaas, Z. M., Mahariq, I., & Sharaf, A. M. (2024). Mitigation uncertainty problems of renewable energy resources with efficient integration of hybrid solar PV/wind system into power networks. *IEEE Access*, *12*, 1–1. https://doi.org/10.1109/access.2024.3370163

Alanazi, A., Alanazi, M., Memon, Z. A., Awan, A. B., & Deriche, M. (2025). Availability and uncertainty-aware optimal placement of capacitors and DSTATCOM in distribution network using improved exponential distribution optimizer. *Scientific Reports*, *15*(1). https://doi.org/10.1038/s41598-025-87139-9

Albadi, M. H., & El-Saadany, E. F. (2008). A summary of demand response in electricity markets. *Electric Power Systems Research*, *78*(11), 1989–1996. https://doi.org/10.1016/j.epsr.2008.04.002

Chen, H., Gao, L., & Zhang, Z. (2021). Multi-objective optimal scheduling of a microgrid with uncertainties of renewable power generation considering user satisfaction. *International Journal of Electrical Power & Energy Systems*, *131*, 107142. https://doi.org/10.1016/j.ijepes.2021.107142

Chuang, M.-T., Chang, S.-Y., Hsiao, T.-C., Lu, Y.-R., & Yang, T.-Y. (2019). Analyzing major renewable energy sources and power stability in Taiwan by 2030. *Energy Policy*, *125*, 293–306. https://doi.org/10.1016/j.enpol.2018.10.036

De, M., & Mandal, K. K. (2022). Energy management strategy and renewable energy integration within multi-microgrid framework utilizing multi-objective modified personal best particle swarm optimization. *Sustainable Energy Technologies and Assessments*, *53*, 102410. https://doi.org/10.1016/j.seta.2022.102410

Deng, X., & Lv, T. (2020). Power system planning with increasing variable renewable energy: A review of optimization models. *Journal of Cleaner Production*, *246*, 118962. https://doi.org/10.1016/j.jclepro.2019.118962

Ebrahimi, H., Shahnia, F., Nikdel, N., & Galvani, S. (2025). Renewable energy and demand uncertainty-aware stochastic allocation and management of soft open points for simultaneous reduction of harmonic distortion, voltage deviations and losses. *Computers and Electrical Engineering*, *123*, 110208. https://doi.org/10.1016/j.compeleceng.2025.110208

Elkadeem, M. R., Abd Elaziz, M., Ullah, Z., Wang, S., & Sharshir, S. W. (2019). Optimal planning of renewable energy-integrated distribution system considering uncertainties. *IEEE Access*, *7*, 164887–164907. https://doi.org/10.1109/access.2019.2947308

Ergun, S., Dik, A., Boukhanouf, R., & Omer, S. (2025). Large-scale renewable energy integration: Tackling technical obstacles and exploring energy storage innovations. *Sustainability*, *17*(3), 1311. https://doi.org/10.3390/su17031311

Feijoo, F., & Das, T. (2015). Emissions control via carbon policies and microgrid generation: A bilevel model and pareto analysis. *Energy*, *90*, 1545–1555. https://doi.org/10.1016/j.energy.2015.06.110

Gangil, G., Saraswat, A., & Goyal, S. K. (2025). An uncertainty aware optimal energy management model for smart distribution networks contemplating reactive support from VRE and energy storage systems. *IEEE Access*, *13*, 1–1. https://doi.org/10.1109/access.2025.3573197

Gharehveran, S. S., Shirini, K., Khavar, S. C., Mousavi, S. H., & Abdolahi, A. (2024). Deep learning-based demand response for short-term operation of renewable-based microgrids. *The Journal of Supercomputing*, *80*(18), 26002–26035. https://doi.org/10.1007/s11227-024-06407-z

Guzmán-Henao, J. A., Bolaños, R. I., Montoya, O. D., Grisales-Noreña, L. F., & Chamorro, H. R. (2024). On integrating and operating distributed energy resources in distribution networks: A review of current solution methods, challenges, and opportunities. *IEEE Access*, *12*, 55111–55133. https://doi.org/10.1109/access.2024.3387400

Hafeez, G., Wadud, Z., Khan, I. U., Khan, I., Shafiq, Z., Usman, M., & Khan, M. U. A. (2020). Efficient energy management of IoT-enabled smart homes under price-based demand response program in smart grid. *Sensors*, *20*(11), 3155. https://doi.org/10.3390/s20113155

Huo, X., Huang, H., Davis, K. R., Poor, H. V., & Liu, M. (2024). A review of scalable and privacy-preserving multi-agent frameworks for distributed energy resources. *Advances in Applied Energy*, 100205–100205. https://doi.org/10.1016/j.adapen.2024.100205

Ibad, M., Barrett, E., & Mason, K. (2025). Uncertainty-aware knowledge transformers for peer-to-peer energy trading with multi-agent reinforcement learning. *arXiv preprint*. https://arxiv.org/pdf/2507.16796

Jiang, Q., Xue, M., & Geng, G. (2013). Energy management of microgrid in grid-connected and stand-alone modes. *IEEE Transactions on Power Systems*, *28*(3), 3380–3389. https://doi.org/10.1109/tpwrs.2013.2244104

Jogunola, O., Ajagun, A. S., Tushar, W., Olatunji, F. O., Yuen, C., Morley, C., Adebisi, B., & Shongwe, T. (2024). Peer-to-peer local energy market: Opportunities, barriers, security and implementation options. *IEEE Access*, *12*, 1–1. https://doi.org/10.1109/access.2024.3375525

Keck, F., Lenzen, M., Vassallo, A., & Li, M. (2019). The impact of battery energy storage for renewable energy power grids in Australia. *Energy*, *173*, 647–657. https://doi.org/10.1016/j.energy.2019.02.053

Konneh, D., Howlader, H., Shigenobu, R., Senjyu, T., Chakraborty, S., & Krishna, N. (2019). A multi-criteria decision maker for grid-connected hybrid renewable energy systems selection using multi-objective particle swarm optimization. *Sustainability*, *11*(4), 1188. https://doi.org/10.3390/su11041188

Lechl, M., Kilian, A., & de Meer, H. (2025). Uncertainty-aware scheduling of multi-use battery storage systems. *Proceedings of the 2025 ACM International Conference on Future Energy Systems (e-Energy)*, 243–256. https://doi.org/10.1145/3679240.3734607

Liou, H. (2010). Policies and legislation driving taiwan's development of renewable energy. *Renewable and Sustainable Energy Reviews*, *14*(7), 1763–1781.

Liu, Z., Ma, L., Wang, K., Zhang, J., Si, C., Yi, J., & Mu, C. (2025). Uncertainty-aware model-based multi-agent deep reinforcement learning for robust active voltage control. *IEEE Transactions on Circuits and Systems I: Regular Papers*, 1–12. https://doi.org/10.1109/tcsi.2025.3588231

Lv, T., & Ai, Q. (2016). Interactive energy management of networked microgrids-based active distribution system considering large-scale integration of renewable energy resources. *Applied Energy*, *163*, 408–422. https://doi.org/10.1016/j.apenergy.2015.10.179

Manoz, K., Rao, A. K., & Rao, R. S. (2025). A multi-objective hybrid meta-heuristic method-based optimal placement of UPFC in power system. *Electrical Engineering*. https://doi.org/10.1007/s00202-025-02985-0

Mokaramian, E., Siano, P., Calderaro, V., Galdi, V., Graber, G., & Ippolito, L. (2024). Innovative peer-to-peer energy trading in local energy communities featuring electric vehicle charging infrastructure. *2024 AEIT International Annual Conference (AEIT)*, 1–6. https://doi.org/10.23919/aeit63317.2024.10736882

Nazemi, M., Dehghanian, P., Lu, X., & Chen, C. (2021). Uncertainty-aware deployment of mobile energy storage systems for distribution grid resilience. *IEEE Transactions on Smart Grid*, *12*(4), 3200–3214. https://doi.org/10.1109/tsg.2021.3064312

Nguyen, T. L., & Nguyen, Q. A. (2025). A multi-objective PSO-GWO approach for smart grid reconfiguration with renewable energy and electric vehicles. *Energies*, *18*(8), 2020. https://doi.org/10.3390/en18082020

Pang, L., Senol, A., Wang, H.-Y., Lai, H.-C., Chuang, K.-T., & Liu, H. (2024). Uncertainty-aware critic augmentation for hierarchical multi-agent ev charging control. *arXiv preprint*. https://arxiv.org/pdf/2412.18047

Parvin, M., Yousefi, H., & Noorollahi, Y. (2023). Techno-economic optimization of a renewable micro grid using multi-objective particle swarm optimization algorithm. *Energy Conversion and Management*, *277*, 116639. https://doi.org/10.1016/j.enconman.2022.116639

Perez-Flores, A. C., Mina, J. D., Olivares-Peregrino, V. H., Jimenez-Grajales, H. R., Claudio-Sanchez, A., & Vicente, G. (2021a). Microgrid energy management with asynchronous decentralized particle swarm optimization [Duplicate entry removed; see Perez-Flores et al. (2021b) for identical content.]. *IEEE Access*, *9*, 69588–69600. https://doi.org/10.1109/access.2021.3078335

Perez-Flores, A. C., Mina, J. D., Olivares-Peregrino, V. H., Jimenez-Grajales, H. R., Claudio-Sanchez, A., & Vicente, G. (2021b). Microgrid energy management with asynchronous decentralized particle swarm optimization. *IEEE Access*, *9*, 69588–69600. https://doi.org/10.1109/access.2021.3078335

Roudnil, S., et al. (2025a). Energy management of microgrids: An MPC-based techno-economic optimisation for RES integration and ESS utilisation. *IET Generation, Transmission & Distribution*, *19*(1), e70082. https://doi.org/10.1049/gtd2.70082

Roudnil, S., et al. (2025b). Enhancing multimicrogrid resilience: A state-of-the-art survey on model predictive control-based energy management strategies. *International Journal of Energy Research*, *2025*(1), 9088459. https://doi.org/10.1155/er/9088459

Roudnil, S., et al. (2025c). A real-time two-step multi-objective planning framework for resilience improvement of islanded microgrids based on MPC. *Journal of Energy Storage*, *119*, 116343. https://doi.org/10.1016/j.est.2025.116343

Sadeghi, R., Sadeghi, S., Memari, A., Rezaeinejad, S., & Hajian, A. (2024). A peer-to-peer trading model to enhance resilience: A blockchain-based smart grids with machine learning analysis towards sustainable development goals. *Journal of Cleaner Production*, *450*, 141880. https://doi.org/10.1016/j.jclepro.2024.141880

Serra, F. M. (2025). Planning, operation and control of microgrids. *Energies*, *18*(7), 1786. https://doi.org/10.3390/en18071786

Sharma, D., & Pindoriya, N. M. (2024). An emission and uncertainty aware optimal dispatch of multi-energy hub. *2022 IEEE PES Innovative Smart Grid Technologies - Asia (ISGT Asia)*, 1–6. https://doi.org/10.1109/isgtasia61245.2024.10876227

Shayeghi, H., & Faraji Davoudkhani, I. (2025). Uncertainty aware energy management in microgrids with integrated electric bicycle charging stations and green certificate market. *Scientific Reports*, *15*(1). https://doi.org/10.1038/s41598-025-12328-5

Soroudi, A., & Amraee, T. (2013). Decision making under uncertainty in energy systems: State of the art. *Renewable and Sustainable Energy Reviews*, *28*, 376–384. https://doi.org/10.1016/j.rser.2013.08.039

Soto, E. A., Bosman, L. B., Wollega, E., & Leon-Salas, W. D. (2021). Peer-to-peer energy trading: A review of the literature. *Applied Energy*, *283*, 116268. https://doi.org/10.1016/j.apenergy.2020.116268

Tarnate, W., Ponci, F., & Monti, A. (2022). Uncertainty-aware model predictive control for residential buildings participating in intraday markets. *IEEE Access*, *10*, 7834–7851. https://doi.org/10.1109/ACCESS.2022.3140598

Thakar, S., A.S., V., & Doolla, S. (2019). System reconfiguration in microgrids. *Sustainable Energy, Grids and Networks*, *17*, 100191. https://doi.org/10.1016/j.segan.2019.100191

Tostado-Véliz, M., Kamel, S., Hasanien, H. M., Turky, R. A., & Jurado, F. (2022). Uncertainty-aware day-ahead scheduling of microgrids considering response fatigue: An IGDT approach. *Applied Energy*, *310*, 118611. https://doi.org/10.1016/j.apenergy.2022.118611

Wang, C., Zhang, Z. G., Abedinia, O., & Farkoush, S. G. (2021). Modeling and analysis of a microgrid considering the uncertainty in renewable energy resources, energy storage systems and demand management in electrical retail market. *Journal of Energy Storage*, *33*, 102111. https://doi.org/10.1016/j.est.2020.102111

Wang, T., Liu, H., & Su, M. (2025). Energy optimization for microgrids based on uncertainty-aware deep deterministic policy gradient. *Processes*, *13*(4), 1047. https://doi.org/10.3390/pr13041047

Wang, Y., Huang, Z., Shahidehpour, M., Lai, L. L., Wang, Z., & Zhu, Q. (2020). Reconfigurable distribution network for managing transactive energy in a multi-microgrid system. *IEEE Transactions on Smart Grid*, *11*(2), 1286–1295. https://doi.org/10.1109/tsg.2019.2935565

Wang, Z., Yu, X., Mu, Y., & Jia, H. (2020). A distributed peer-to-peer energy transaction method for diversified prosumers in urban community microgrid system. *Applied Energy*, *260*, 114327. https://doi.org/10.1016/j.apenergy.2019.114327

Wongthongtham, P., Marrable, D., Abu-Salih, B., Liu, X., & Morrison, G. (2021). Blockchain-enabled peer-to-peer energy trading. *Computers & Electrical Engineering*, *94*, 107299. https://doi.org/10.1016/j.compeleceng.2021.107299

Xiao, H., Du, Y., Pei, W., & Kong, L. (2017). Coordinated economic dispatch and cost allocation of cooperative multi-microgrids. *The Journal of Engineering*, *2017*(13), 2363–2367. https://doi.org/10.1049/joe.2017.0753

Xu, C., & Abdalla, A. (2026). Coordinated dispatch of electric, thermal, and hydrogen vectors in renewable-enriched microgrids using constrained harris hawks optimization under uncertainty. *Renewable Energy*, *256*, 124064. https://doi.org/10.1016/j.renene.2025.124064

Xu, Y., Yu, L., Bi, G., Zhang, M., & Shen, C. (2020). Deep reinforcement learning and blockchain for peer-to-peer energy trading among microgrids. *2020 IEEE International Conference on Internet of Things and Intelligence System (IoTaIS)*. https://doi.org/10.1109/ithings-greencom-cpscom-smartdata-cybermatics50389.2020.00071

Zare, K., Akbari-Dibavar, A., Najafi Ravadanegh, S., & Vahidinasab, V. (2024). Resiliency-oriented scheduling of multi-microgrids in the presence of fuel cell-based mobile storage using hybrid stochastic-robust optimization. *Journal of Energy Management and Technology*, *8*(4), 307–320. https://doi.org/10.22109/jemt.2024.441626.1487

Zhang, C., Yang, T., & Wang, Y. (2021). Peer-to-peer energy trading in a microgrid based on iterative double auction and blockchain. *Sustainable Energy, Grids and Networks*, *27*, 100524. https://doi.org/10.1016/j.segan.2021.100524

Zhang, W., Bao, X., Hao, X., & Gen, M. (2025). Metaheuristics for multi-objective scheduling problems in industry 4.0 and 5.0: A state-of-the-arts survey. *Frontiers in Industrial Engineering*, *3*. https://doi.org/10.3389/fieng.2025.1540022

Zhang, X., Zhou, Y., Ge, S., Liu, H., & Yang, B. (2024). Data-driven stochastic planning for network constrained energy sharing in microgrids. *2024 IEEE Power & Energy Society General Meeting (PESGM)*, 1–5. https://doi.org/10.1109/pesgm51994.2024.10688976

Zhang, Y., Tian, J., Guo, Z., Fu, Q., & Jing, S. (2025). Uncertainty-aware economic dispatch of integrated energy systems with demand-response and carbon-emission costs. *Processes*, *13*(6), 1906. https://doi.org/10.3390/pr13061906

Zhang, Y., Wang, S., & Ji, G. (2015). A comprehensive survey on particle swarm optimization algorithm and its applications. *Mathematical Problems in Engineering*, *2015*, 1–38. https://doi.org/10.1155/2015/931256

Zhou, B., Zou, J., Yung Chung, C., Wang, H., Liu, N., Voropai, N., & Xu, D. (2021). Multi-microgrid energy management systems: Architecture, communication, and scheduling strategies. *Journal of Modern Power Systems and Clean Energy*, *9*(3), 463–476. https://doi.org/10.35833/mpce.2019.000237

Zhou, F., & Yu, R. (2025). Moving edge for on-demand edge computing: An uncertainty-aware approach. *arXiv preprint arXiv:2503.24214*.

Zhou, H., Yuan, F., Guo, L., & Gan, M. (2025). Integrating stacking-ensemble feature selection with GRU-based self-supervised learning for precision and uncertainty-aware steam flow forecasting. *SSRN*. https://doi.org/10.2139/ssrn.5188272

Zubin, J., Sunitha, R., & Pathirikkat, G. (2025). Integrated bidding and battery scheduling in a microgrid for sealed-bid double auction power trading with peer microgrids under uncertainty and its blockchain-based implementation [Preprint]. *IEEE Access*. https://doi.org/10.1109/ACCESS.2025.3586465